

ORIGINAL ARTICLE

Salvianolic acid B inhibits thrombosis and directly blocks the thrombin catalytic site

Miguel A. D. Neves^{1,2,3,4} | Tiffany T. Ni^{1,2,3} | Daniel T. Mackeigan^{2,3,5} |
Aron A. Shoara^{2,3,4,5,6} | Xi Lei^{2,3} | Sladjana Slavkovic^{2,3,4} | Si-Yang Yu^{2,3} |
Tyler W. Stratton^{1,2,3} | Reid C. Gallant^{1,2,3} | Dan Zhang^{2,3} |
Xiaohong Ruby Xu^{1,2,3,4} | Cheryl Fernandes^{2,3} | Guangheng Zhu^{2,3,4} |
Xudong Hu^{2,3} | Noa Chazot^{1,2,3} | Logan W. Donaldson⁶ | Philip E. Johnson⁶ |
Kim Connelly^{2,5,7,13} | Margaret Rand^{1,3,8,9} | Yiming Wang^{1,2,3,4,10,11,12} |
Heyu Ni^{1,2,3,4,5,13}

¹Department of Laboratory Medicine and Pathobiology, University of Toronto, Toronto, Ontario, Canada

²Keenan Research Centre for Biomedical Science, St. Michael's Hospital, Toronto, Ontario, Canada

³Toronto Platelet Immunobiology Group, University of Toronto, Toronto, Ontario, Canada

⁴Canadian Blood Services Centre for Innovation, Toronto, Ontario, Canada

⁵Department of Physiology, University of Toronto, Toronto, Ontario, Canada

⁶Department of Chemistry and Centre for Research on Biomolecular Interactions, York University, Toronto, Ontario, Canada

⁷Division of Cardiology, St. Michael's Hospital, Toronto, Ontario, Canada

⁸Division of Hematology, The Hospital for Sick Children, Toronto, Ontario, Canada

⁹Department of Biochemistry, University of Toronto, Toronto, Ontario, Canada

¹⁰Division of Clinical and Metabolic Genetics, The Hospital for Sick Children, Toronto, Ontario, Canada

¹¹Genetics and Genome Biology Program, Peter Gilgan Centre for Research and Learning, Toronto, Ontario, Canada

¹²Department of Paediatrics, University of Toronto, Toronto, Ontario, Canada

¹³Department of Medicine, University of Toronto, Toronto, Ontario, Canada

Correspondence

Yiming Wang, Division of Clinical and Metabolic Genetics, The Hospital for Sick Children, Department of Paediatrics, University of Toronto, 555 University Avenue, Toronto, ON M5G 2L3, Canada.
Email: yiming.wang@sickkids.ca

Heyu Ni, Department of Laboratory Medicine and Pathobiology, Department of Medicine, and Department of Physiology, University of Toronto, Canadian Blood Services, Cancer and Immunological Diseases, St. Michael's Hospital, Room 420,

Abstract

Background: Salvianolic acid B (SAB) is a major component of *Salvia miltiorrhiza* root (Danshen), widely used in East/Southeast Asia for centuries to treat cardiovascular diseases. Danshen depside salt, 85% of which is made up of SAB, is approved in China to treat chronic angina. Although clinical observations suggest that Danshen extracts inhibited arterial and venous thrombosis, the exact mechanism has not been adequately elucidated.

Objective: To delineate the antithrombotic mechanisms of SAB.

Methods: We applied platelet aggregation and coagulation assays, perfusion chambers,

Miguel A. D. Neves, Tiffany T. Ni, and Daniel T. Mackeigan contributed equally to this study.

Some of the data from this work have been orally presented at the 2019 American Heart Association Scientific Sessions and the 27th International Society on Thrombosis and Haemostasis Congress. This manuscript has not been submitted for publication in any other scientific journal.

© 2024 The Authors. Published by Elsevier Inc. on behalf of International Society on Thrombosis and Haemostasis. This is an open access article under the CC BY-NC-ND license (<http://creativecommons.org/licenses/by-nc-nd/4.0/>).

LKSKI - Keenan Research Centre, 209
Victoria Street, Toronto, ON M5B 1T8,
Canada.
Email: heyu.ni@unityhealth.to

Handling Editor: Henri Spronk

and intravital microscopy models. The inhibition kinetics and binding affinity of SAB to thrombin are measured by thrombin enzymatic assays, intrinsic fluorescence spectrophotometry, and isothermal titration calorimetry. We used molecular *in silico* docking models to predict the interactions of SAB with thrombin.

Results: SAB dose-dependently inhibited platelet activation and aggregation induced by thrombin. SAB also reduced platelet aggregation induced by adenosine diphosphate and collagen. SAB attenuated blood coagulation by modifying fibrin network structures and significantly decreased thrombus formation in mouse cremaster arterioles and perfusion chambers. The direct SAB-thrombin interaction was confirmed by enzymatic assays, intrinsic fluorescence spectrophotometry, and isothermal titration calorimetry. Interestingly, SAB shares key structural similarities with the trisubstituted benzimidazole class of thrombin inhibitors, such as dabigatran. Molecular docking models predicted the binding of SAB to the thrombin active site.

Conclusion: Our data established SAB as the first herb-derived direct thrombin catalytic site inhibitor, suppressing thrombosis through both thrombin-dependent and thrombin-independent pathways. Purified SAB may be a cost-effective agent for treating arterial and deep vein thrombosis.

KEYWORDS

blood coagulation, platelet, salvianolic acid B (SAB), thrombin, thrombosis

Essentials

- Danshen, with its main ingredient salvianolic acid B (SAB), is widely used in Asia to treat cardiovascular diseases.
- Danshen depside salt has a potent clinical antithrombotic effect, but the mechanism is unclear.
- SAB inhibits platelet function and coagulation via thrombin-dependent and thrombin-independent pathways.
- SAB shares structural similarities with dabigatran and directly blocks thrombin catalytic site.

1 | INTRODUCTION

Platelet adhesion, aggregation, and blood coagulation are key processes of hemostasis to protect against blood loss following trauma in humans and other mammals [1–6]. However, when the blood coagulation cascade and platelets are inaptly activated, a similar process of hemostasis may turn toward thrombosis, resulting in occlusion of the blood vessel, ischemia of downstream tissues, and ultimately, heart attack and stroke [7–12]. Thrombotic events may also occur in placentas, leading to miscarriage [13,14]. Thrombotic diseases are estimated to account for 1 in 4 deaths worldwide, and their incidence and mortality rates continue to rise in developing countries, where the risk is aggravated by limited access to newer antithrombotic medications [15].

As a crucial coagulation factor, the serine protease thrombin is generated through the activation of the coagulation cascade and catalyzes the proteolytic conversion of the soluble fibrinogen into the insoluble fibrin clot [16,17]. Thrombin is also a potent agonist for platelet activation by enzymatically activating the platelet surface protease-activated receptors [18–20]. Therefore, thrombin plays a central role in platelet activation, aggregation, and blood coagulation

and has been an attractive target for the development of antithrombotic agents for decades [21]. It was only about a decade ago that the first inhibitor of the thrombin active site, dabigatran, was approved for clinical use [22]. However, the high price of dabigatran and other new antithrombotic agents has significantly limited their use in developing countries, where a surge in thrombosis-related mortality and morbidity occurs [23].

Danshen, a traditional Chinese medicine, has long been used in East and Southeast Asia for its antithrombotic, antiinflammatory, and antimicrobial properties [24,25]. Danshen depside salt has been approved by the Chinese State Food and Drug Administration to treat coronary heart disease and is one of the most commonly used traditional Chinese medicines [26]. In China alone, Danshen depside has been used in over 450 million patients since entering the market in 1994, although its exact mechanism of action is poorly understood [27]. Salvianolic acid B (SAB) makes up over 85% of Danshen depside salt and is the main active antithrombotic component of Danshen [28]. Considering the current large-scale clinical use of SAB in Asia, there is an urgency to understand its mechanisms of action to maximize benefits and prevent complications. With its potent clinical

antithrombotic effect, SAB was proposed to interact with platelet P2Y1, P2Y12, and $\alpha 2\beta 1$ integrin and moderately inhibited platelet aggregation and adhesion [29–31]. However, whether these interactions represent the predominant mechanisms for the inhibitory effect of SAB on thrombus formation is unknown. In addition, the impact of SAB on blood coagulation has never been previously explored.

In this study, we investigated the role of SAB in platelet aggregation and blood coagulation. Our findings established SAB as a direct competitive inhibitor of thrombin.

2 | METHODS

2.1 | Platelet aggregation assay

Human platelet aggregation in platelet-rich plasma and piperazine-*N,N'*-bis-2-ethanesulfonic acid buffer was performed as we previously described [32–35]. Platelet aggregation was induced by 0.02 U/mL bovine thrombin (Sigma–Aldrich), 5 $\mu\text{g}/\text{mL}$ collagen (Chrono-Log), or 20 μM adenosine diphosphate (ADP, Sigma–Aldrich) utilizing a computerized aggregometer (Chrono-Log) with the stir bar rate set to 1000 rpm at 37 °C. Platelet concentrations were determined with a Coulter Counter and adjusted to a final concentration of 3.0×10^8 platelets/mL. Platelets were incubated with SAB solutions in phosphate-buffered saline (PBS; 10 mM sodium phosphate buffer, 2.7 mM KCl, 137 mM NaCl, pH 7.4) in a concentration range from 0.1 to 0.3 mM SAB or control PBS buffer for 10 minutes at 37 °C. The change in light transmission was recorded for a minimum of 8 minutes.

2.2 | Clot formation assay

Clot formation assay was performed as we previously described [33,36]. Mouse blood (from the inferior vena cava) and human blood samples were individually drawn into 3.2% (w/v) sodium citrate at 9:1 volume ratio. The blood samples were then diluted 3 times and treated with a final concentration of 0.3 mM SAB in PBS or an equal volume of blank PBS. All samples were recalcified with 1 mM CaCl_2 and 2 U/mL thrombin and incubated at 37 °C for 90 minutes. The clot was then removed from the serum, and dry weight was measured after 24 hours at room temperature (20 °C).

2.3 | Prothrombin time and activated partial thromboplastin time measurement

For prothrombin time (PT) measurements, 20 mL of RecombiPlasTin 2G (HemosIL) and RecombiPlasTin2G diluent were incubated for 20 minutes at room temperature and mixed in a 1:1 ratio as previously described [37,38]. The reconstituted mixture was then incubated at 37 °C for 5 minutes. A steel ball was placed in each cuvette, and 50 μL of human platelet-poor plasma (PPP) was then added to each cuvette.

Once 100 μL of reconstituted RecombiPlasTin 2G was added to each cuvette, the test was immediately started and concluded with the formation of a solid gel. For activated partial thromboplastin time measurements, SynthASil was mixed well, and both SynthASil and 20 mM CaCl_2 were incubated at room temperature for 20 minutes. Fifty microliters of SynthASil was added to the cuvette and incubated for 2 minutes at 37 °C. After adding 50 μL of 20 mM CaCl_2 , the test immediately started and was completed with the formation of a solid gel.

2.4 | Clot turbidity assay

The coagulation turbidity assay was conducted on human PPP following a previously established method [39,40]. Aliquots of frozen PPP samples stored in -20 °C for less than a week were thawed at room temperature. Human PPP and SAB were preincubated for 10 minutes and then mixed with 50 mM CaCl_2 and 0.1 U/mL thrombin in a Thermo Scientific Nunc MicroWell 96-Well microplate to a final volume of 100 μL . The microplate was then placed in a BioTek Synergy Neo plate reader at 37 °C that rigorously mixed the plate for 15 seconds and then monitored the absorbance at 405 nm until all conditions plateaued.

2.5 | Thromboelastography

The thromboelastography (TEG) assay was performed as we previously described [33]. Blood from healthy human donors in 3.2% sodium citrate was tested in a TEG 5000 Analyzer (Hemoscope) following recalcification with 0.2 M calcium chloride. The blood was treated with either 0.3 mM of SAB or an equal volume of PBS.

2.6 | Confocal laser scanning and scanning electron microscopy

Fibrin clot formation was performed as previously described [33]. The fibrin network was formed by combining 5 μL of human PPP with 1 μL of unlabeled Fg and Alexa-488-labeled Fg mixture (40:1 ratio; total final concentration, 1 mg/mL; Sigma–Aldrich). Samples were then calcified with 1.5 μL of 0.2 M CaCl_2 and incubated with SAB and blank PBS in the control group. Finally, 4 μL of 50 U/mL of bovine thrombin was added, and slides were incubated at room temperature for 30 minutes in a humidity chamber. Slides were imaged on a Zeiss LSM 700 microscope using a 40 \times water immersion objective at room temperature and processed using Imaris software (Bitplane). Fibrin network formation was prepared as described above using human PPP. The fibrin network was fixed using 2.5% glutaraldehyde (Electron Microscopy Sciences) in 0.1 M sodium phosphate buffer for 1 hour at room temperature. The samples were then washed 3 times for 10 minutes each using 0.1 M sodium phosphate buffer. Samples then underwent gold sputter coating and were mounted on scanning

electron microscopy clips and captured using a scanning electron microscope (Hitachi High-Technologies SU3800/SU3900).

2.7 | Perfusion chamber analysis

Perfusion chamber analysis was performed as we previously described [41–44]. Heparin (5 U/mL) anticoagulated human whole blood was perfused over the collagen-coated glass chamber surface at controlled shear rates (1800 s^{-1} and 300 s^{-1}) for 3 minutes using a syringe pump individually. The thrombus formation was captured by confocal microscopy. Human whole blood was labeled with $1 \mu\text{M}$ 3,3'-dihexyloxycarbocyanine iodide (DiOC₆, Sigma–Aldrich) for 20 minutes at 37°C and then incubated with SAB or PBS control for 10 minutes. Platelet adhesion was recorded over the course of perfusion under a Zeiss Axiovert 135 inverted fluorescence microscope (IBM IntelliStation Z Pro). Mean fluorescence intensity (MFI) was analyzed using the Slidebook program (Intelligent Imaging Innovations).

2.8 | Intravital microscopy thrombosis model

Intravital microscopy was performed as we previously described [45–47]. Dylight 488-labeled pFn (5 μg) anti-GPIb antibodies (1 $\mu\text{g/g}$ body weight) were injected through the jugular vein cannula prior to the injury. SAB was injected through the jugular vein cannula to a final *in vivo* concentration of 0.010 mM based on the weight of each mouse (80 $\mu\text{L/g}$ total blood volume). Multiple independent injuries were induced on cremaster arterioles using an Olympus BX51W1 microscope equipped with a pulsed nitrogen dye laser. The dynamic formation of the hemostatic plug was captured and analyzed using Slidebook software (Intelligent Imaging Innovations).

2.9 | Ferric chloride carotid artery thrombosis model

Carotid artery injury was induced as we previous described [34]. A strip of Whatman filter paper saturated with 10% ferric chloride was applied onto the exposed adventitia for 180 seconds in isoflurane-anesthetized C57BL/6J mice (aged >8 weeks, 20–35 g). The vessel was then rinsed with warm physiologic saline solution and the flow rate was measured for 30 minutes with a miniature Doppler flow probe (TS420 transit-time perivascular flowmeter, Transonic Systems Inc). At the time of 50% reduction of the carotid flow, either normal saline or 15 milligrams per kilogram (mpk) of SAB was injected through the tail vein (corresponding to $\sim 0.3 \text{ mM}$ final blood concentration of SAB). The rescue of the carotid blood flow rate and occlusion time was documented.

2.10 | Isothermal titration calorimetry

Isothermal titration calorimetry (ITC) binding experiments were performed using a MicroCal VP-ITC instrument at 20°C in PBS buffer (pH 7.4) as we previously described [25,48,49]. SAB and thrombin were prepared in PBS, while dabigatran stock was prepared in 100% dimethyl sulfoxide (DMSO) and diluted to experimental concentrations with buffer to a final DMSO concentration of 1% (v/v). DMSO was added to the thrombin solution and the reference cell at the same concentration to avoid buffer mismatch. Titrations were performed with the small molecule ligand samples in the cell and the protein as the titrant in the instrument syringe. The binding experiments involving thrombin were performed with the small molecule ligand solutions ranging from 10 to 20 μM using a protein concentration of 150 μM . ITC binding experiments consisted of an initial delay of 60 seconds, first purge injection of 2 μL , and subsequent 20 injections of 14 μL , spaced every 300 seconds between every injection. Titration of SAB into lysozyme was performed with lysozyme (20 μM) in the cell and SAB (0.312 mM) as the titrant in the syringe. The binding experiments involving lysozyme consisted of an initial delay of 60 seconds, first purge injection of 2 μL and subsequent 34 injections of 8 μL , also spaced every 300 seconds. The first point was removed from all data sets due to the difference in injection volume. All experiments were corrected for the heat of dilution of the titrant obtained from analyte-to-buffer titrations. SAB binding to thrombin was fitted to a 2-site cooperative binding model developed by Freiburger et al. [50] using MATLAB 14 software, while dabigatran binding to thrombin was fitted to a 2-site independent binding model using supplied Origin 7 software [48]. Hill coefficient (n_H) was determined using the established methods [51,52].

2.11 | Fluorescence spectrophotometry analysis

The intrinsic fluorescence of SAB was analyzed in PBS employing a Cary Eclipse fluorescence spectrophotometer and 10-mm fused quartz cuvettes. The temperature was maintained constant throughout each experiment at 20°C using a Cary Peltier controller. The spectrofluorometer was optimized for the limit of detection to maintain constant photomultiplier tube voltage, signal-to-noise ratio, and spectral bandwidth parameters, and the inner-filter effect for the loss of the excitation light intensity was calculated as we previously described [35,53]. Optimized intrinsic fluorescence properties of unbound SAB in PBS were obtained at 382 nm excitation wavelength with a maximum emission peak at $498 \pm 1 \text{ nm}$. Next, $29.4 \pm 0.5 \mu\text{M}$ SAB was titrated with thrombin from 0 to $71.6 \pm 0.1 \mu\text{M}$. For negative controls, we titrated $27.2 \pm 0.4 \mu\text{M}$ SAB with lysozyme from 0 to $95.6 \pm 0.1 \mu\text{M}$ and a blank PBS buffer separately, in the same manner as described for thrombin. Observed integrated SAB fluorescence emission intensities were averaged, normalized, and plotted vs the titrant protein concentrations to quantify the apparent dissociation constant (K_d) value. Each

experiment was performed in 4 trials and analyzed using our previously published binding model (OriginLab 2016) [54].

2.12 | Thrombin activity assay

We examined the effect of SAB on the enzymatic activity of 0.1 U/mL human thrombin in a fluorogenic assay of n-benzoyl-Phe-Val-Arg 7-amido-4-methylcoumarin (Sigma-Aldrich) as substrate utilizing a BioTek Synergy Neo plate reader and its corresponding software. We measured fluorescence signal propagation of 7-amino-4-methylcoumarin at $\lambda_{\text{ex}} = 320$ nm and $\lambda_{\text{em}} = 420$ nm as a function of time and quantified the initial rate (V_0) of thrombin activity in a concentration range of 0 to 0.1 mM substrate and a concentration range of 0 to 0.1 mM SAB in PBS (pH 7.4) at 25 °C. The average initial rate values from triplicated experiments were plotted as a function of substrate concentration and analyzed using a global Michaelis-Menten binding model to quantify thrombin activity parameters of K_M , K_i , and V_{max} [34,55].

2.13 | Molecular modeling and docking

We analyzed the tertiary structure of the binding pocket of human thrombin bound to trisubstituted benzimidazole inhibitor and SAB. We used AutoDock Vina 1.2.0 scripts [56] and the available X-ray crystal structure of the thrombin-inhibitor complex with 2.40 Å resolution [57] and the SAB structure. We clustered the obtained results with maximum root mean square deviation values of 2.0 and compared them for optimal binding efficiency based on the quantified binding energies. We then rendered structures with the lowest binding energy values (kcal/mol) in PyMol (Schrodinger, LLC) for bond length measurements and visualization [58,59].

2.14 | Statistical analysis

GraphPad Prism 10 was used for all statistical analysis. Statistical significance was assessed with paired or unpaired t-test (2-tailed). When a 1-way ANOVA for nonrepeated measures was performed, Dunnett's post hoc test was used to compare between treatments and control. All data are presented as mean \pm SEM unless stated otherwise. Data were determined to be statistically significant when $P < .05$.

3 | RESULTS

3.1 | SAB blocks thrombin-induced platelet aggregation and attenuates platelet aggregation induced by other agonists

Platelet aggregation is the key process for arterial thrombosis and contributes to venous thrombosis [2,10]. We first examined the effect

of SAB on platelet aggregation. Human gel-filtered platelet aggregation induced by 0.02 U/mL of thrombin was dose-dependently inhibited by SAB with an effective dose concentration (EC_{50}) of 0.044 ± 0.01 mM (Figure 1A, B). At an SAB concentration of 0.16 mM, platelet aggregation was completely abolished (Figure 1A, B). Consistent with these results, we found that SAB inhibits the expression of various human platelet surface activation markers, as shown by flow cytometry (Figure 1C). SAB significantly reduced the thrombin-induced platelet surface expression of P-selectin, *Ricinus communis* agglutinin-1 (RCA-1, an activation marker following platelet desialylation) [60,61], and annexin-V. Notably, the binding of platelet activation complex-1 (PAC-1) monoclonal antibody and fibrinogen is significantly decreased, which indicates a decreased activation of $\alpha\text{IIb}\beta_3$ integrin. SAB also attenuated collagen- and ADP-induced platelet aggregation (Supplementary Figure S1A-D), suggesting that SAB can inhibit both thrombin-dependent and thrombin-independent pathways.

We found that prolonged storage in solution and repeated freeze-thaw cycles lead to decreased SAB inhibitory function for platelet aggregation. Freshly prepared SAB that preserved the optimal function, as shown in this study, has ultraviolet light absorption peaks at 250 nm and 280 nm in spectrophotometry corresponding to benzofuran and catechol functional groups (Supplementary Figure S2A). After prolonged storage and frequent freeze-thaw cycles, inactivated SAB that lost the inhibitory effect showed a distinct peak at 362 nm (Supplementary Figure S2B). We attribute this change to the oxidation process of catechol to benzoquinone. Interestingly, the SAB returns to its active conformation when exchanged in 10% (v/v) trifluoroacetic acid (Supplementary Figure S2B). For our study, all SAB solutions used in experiments were freshly made from SAB powder (Sigma-Aldrich) stored at -20 °C, followed by confirmation of the absorption peaks at 250 nm and 280 nm by spectrophotometry, which we think is crucial for ensuring the optimal biological/therapeutic function of SAB.

3.2 | SAB inhibited blood coagulation *in vitro* and reduced fibrin-fiber density and diameter in the blood clot

The potent suppression of thrombin-induced platelet aggregation by SAB suggests a potential impact of SAB on blood coagulation, which is a cascade of enzymatic reactions leading to the generation of thrombin, which then converts the soluble fibrinogen to an insoluble fibrin-fiber network [16]. We first analyzed the effect of SAB on blood coagulation *in vitro* [33]. In a whole blood clot formation assay, 0.3 mM of SAB significantly reduced the dry weight of the human blood clot (Figure 2A), suggesting defects in clot organization and red blood cell retention. Consistently, 0.6 mM SAB prolonged PT and activated partial thromboplastin time of human cell-free plasma (Figure 2B, C), indicating the inhibitory effect on both intrinsic and extrinsic coagulation pathways. To evaluate the impact of SAB on the kinetics of clot formation, we studied coagulation with a clot turbidity assay. SAB dose-dependently delayed cell-free human blood plasma coagulation

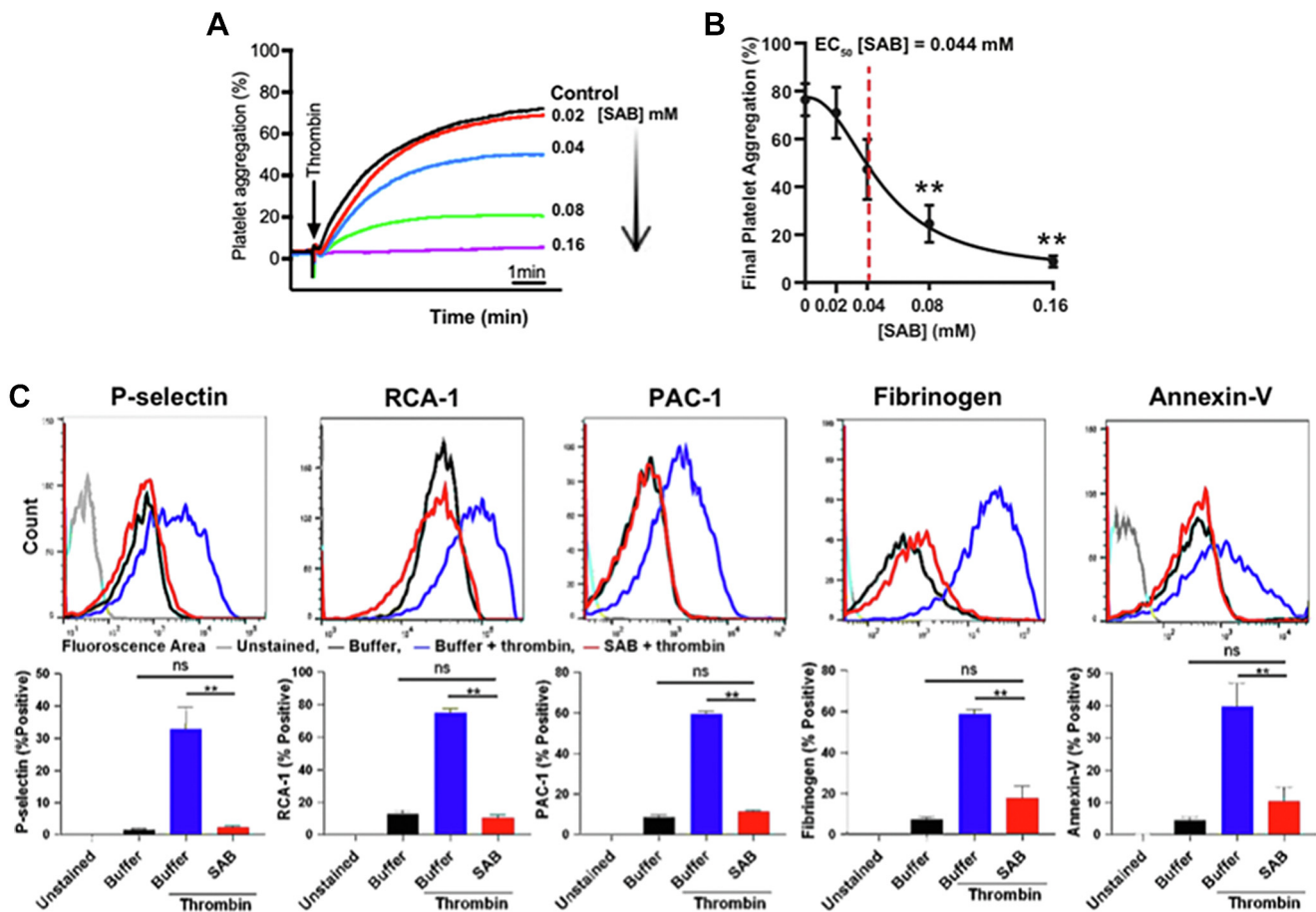


FIGURE 1 SAB inhibits thrombin-induced human platelet aggregation. Human gel-filtered platelet aggregation was induced with 0.02 U/mL thrombin (A, B). Panel A shows a representative single experiment, and panel B displays dose–response and statistical analyses of thrombin-induced aggregation as a function of SAB concentration. The EC_{50} dose is quantified (0.044 ± 0.01 mM SAB, $R^2 = 0.9974$). (C) Human platelet activation analyses using flow cytometry. Platelets were labeled at room temperature for 30 minutes, and 10,000 events were captured on a Fortessa flow cytometer. The analyzed histograms and their corresponding activation markers are shown on top, and statistical analysis is displayed on bottom panels. The black, blue, and red lines indicate the groups of PBS treatment with no agonists, PBS treatment with thrombin, and SAB treatment with thrombin, respectively. ** P value $< .01$, $n = 3-4$. EC_{50} , effective dose concentration; PBS, phosphate-buffered saline; SAB, salvianolic acid B.

with an EC_{50} of (0.062 ± 0.07) mM (Figure 2D, E). SAB (0.3 mM) also significantly prolonged the initiation of human blood coagulation in TEG (Supplementary Figure S3). These data suggest that SAB interacts with the coagulation cascade and suppresses blood clot formation.

To directly visualize the impact of SAB on the clot microstructure, fibrin networks were formed using plasma-free recombinant human fibrinogen with thrombin as an agonist and then visualized under a confocal laser scanning microscopy. SAB significantly decreased the surface coverage of the fluorescently labeled fibrin network formed in a glass chamber (Figure 3A, B), suggesting a direct action on the enzymatic process of the thrombin-induced fibrin network formation. The detailed fibrin–fibrin structure was observed under scanning electron microscopy. We found that SAB modified the microstructure of the fibrin network and the individual fibrin fibers. The fiber diameter was increased while the density was significantly decreased (Figure 3C–E). These parameter changes

were previously reported to be associated with the weakening of the fibrin network [62]. These *in vitro* data demonstrate that SAB attenuated blood coagulation through direct modification of the fibrin network of the clot.

3.3 | SAB attenuated thrombosis in mouse cremaster muscle arterioles and *ex vivo* perfusion chambers

We examined the impact of SAB on thrombus formation *in vivo* using a laser–injury intravital microscopy model [41,45,47]. We found that 0.010 mM of SAB reduced thrombus formation in mouse cremaster vessels by approximately $65 \pm 5\%$ (Figure 4A, B), suggesting a strong antithrombotic effect *in vivo*. In collagen-coated glass chambers [42,44], human platelet thrombus formation was significantly inhibited

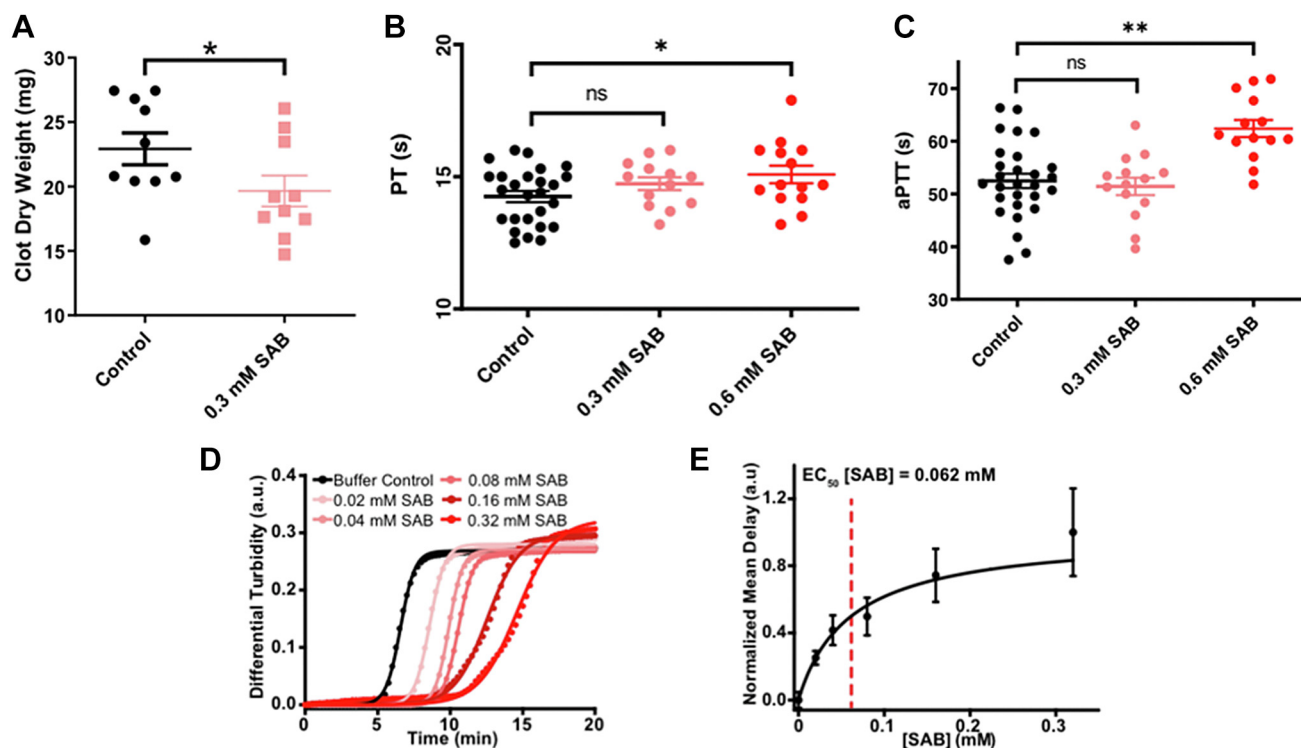


FIGURE 2 SAB inhibits human blood coagulation *in vitro*. (A) SAB decreased the dry weight of clots formed in whole blood. (B, C) SAB prolonged PT and aPTT at 0.6 mM. (D) Delay of blood coagulation in the clot turbidity assay. Superimposed turbidity plots as a function of SAB concentration. Turbidity at 405 nm was used as an indication of coagulation and monitored for 20 minutes at 37 °C. Differential turbidity values were analyzed using a Boltzmann kinetics model. SAB dosages from 0.08 to 0.32 mM were utilized. (E) The measured delay time of blood coagulation plots shown in panel D was analyzed as a function of SAB concentration, where an EC_{50} of 0.062 ± 0.07 mM SAB was quantified (dotted red line), $R^2 = 0.9844$. ** $P < .01$, * $P < .05$. aPTT, activated partial thromboplastin time; PT, prothrombin time; SAB, salvianolic acid B.

by 0.32 mM of SAB under both venous shear rate (300 s^{-1} ; [Supplementary Figure S4A–C](#)) and arterial shear rate (1800 s^{-1} ; [Supplementary Figure S4D–F](#)). SAB also rescued the carotid blood flow and prolonged the vessel occlusion in the ferric chloride carotid artery thrombosis model ([Supplementary Figure 5A, B](#)). These data showed the significant inhibition of thrombosis by SAB *in vivo* and *ex vivo*, providing a mechanism for the potent clinical antithrombotic effect observed in patients.

3.4 | SAB dose-dependently reduced enzymatic activity of thrombin through blocking the thrombin catalytic site

Our *in vitro* and *in vivo* data showed that SAB suppresses platelet aggregation, adhesion, and blood coagulation [57]. The inhibitory effect was particularly potent when thrombin was used as an agonist. Utilizing an enzymatic activity assay for thrombin, we found that SAB dose-dependently inhibited the thrombin protease function with an inhibition constant (K_i) of $1.70 \pm 0.27 \text{ } \mu\text{M}$ ([Figure 5A](#) and [Supplementary Table S1](#)), suggesting a direct inhibition of thrombin by SAB.

To study whether there is direct binding SAB to thrombin using a label-free technique, we utilized steady-state fluorescence spectrophotometry to analyze the binding affinity of SAB-thrombin *in vitro*, which is

the first to report the application of SAB autofluorescence. By measuring the fluorescence intensity change as a function of thrombin concentration, we quantified the apparent dissociation constant of SAB-thrombin as $21.7 \pm 1.5 \text{ } \mu\text{M}$ ([Figure 5B](#)). The apparent dissociation constant confirms the total effect of binding. Upon the titration of thrombin protein in SAB solution, the inherent fluorescence emission of SAB was initially quenched up to $\sim 1 \text{ } \mu\text{M}$ thrombin and then enhanced as thrombin concentration added up to $71.6 \text{ } \mu\text{M}$ ([Figure 5C](#)). We separately titrated SAB with lysozyme and PBS buffer as negative controls, which showed a linear change due to the dilution of SAB ([Supplementary Figure S6A, B](#)), suggesting no direct interactions between lysozyme and SAB. We also examined the stability of SAB bound to thrombin as a function of time and found less than 3% decrease in the SAB-thrombin complex signal after 24 hours at room temperature ([Supplementary Figure S6C](#)).

Using ITC, we revealed a nonsigmoidal binding isotherm for thrombin–SAB titrations, which are consistent with direct binding of SAB to thrombin at 2 distinct binding sites, with a dissociation constant (K_{d1}) of $0.62 \pm 0.08 \text{ } \mu\text{M}$ at the strong binding site and K_{d2} of $37 \pm 4 \text{ } \mu\text{M}$ at the weak binding site ([Figure 5D, Table](#)). In comparison with SAB, dabigatran binds to thrombin with a lower K_{d1} of $0.49 \pm 0.16 \text{ nM}$ and K_{d2} of $24 \pm 13 \text{ nM}$ ([Figure 5E, Table](#)). Furthermore, we used lysozyme as a control and detected no interaction with SAB ([Figure 5F](#)). The thermodynamic analysis of the binding between SAB and thrombin reveals that this ligand forms a complex with an

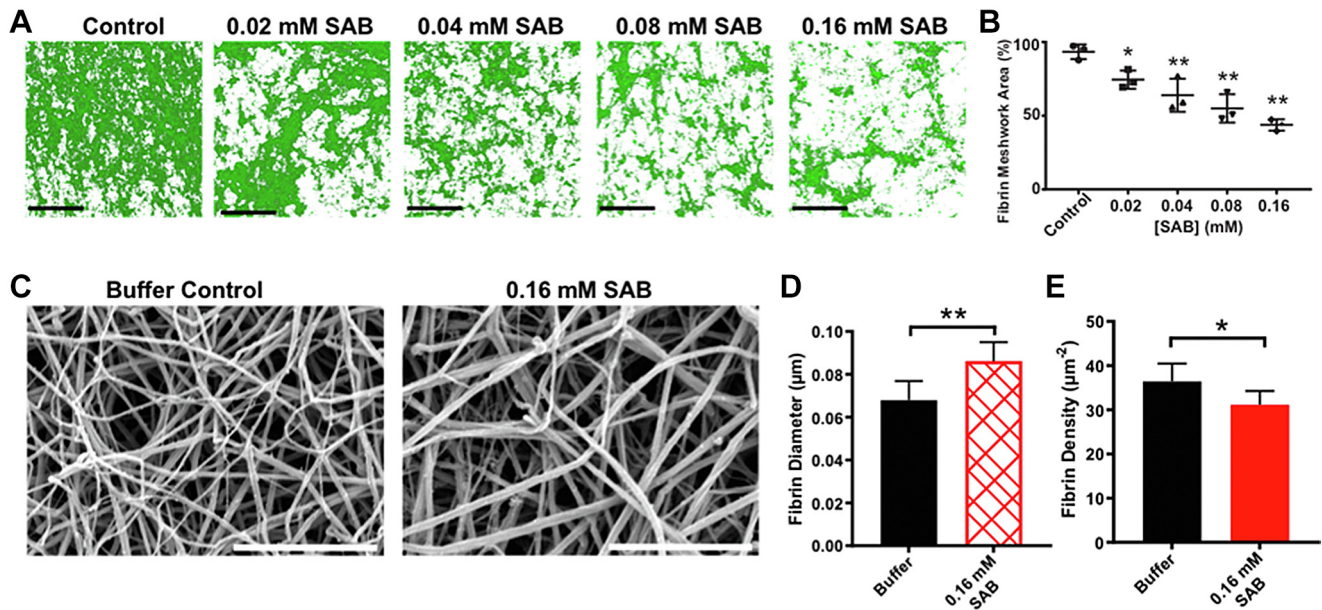


FIGURE 3 SAB reduces thrombin-induced fibrin network formation with rhFg. Human blood coagulation was induced by 0.02 U/mL bovine thrombin in rhFg. (A, B) Dose-dependent inhibition of surface fibrin clot coverage by SAB at dosages from 0.02 mM to 0.16 mM. Each black scale bar signifies 100 microns. (C, D, E) 0.16 mM SAB significantly increased the fibrin-fiber diameter and reduced fiber density. Each white scale bar measures 50 microns. ** $P < .01$, * $P < .05$. rhFg, recombinant human fibrinogen; SAB, salvianolic acid B.

unfavorable enthalpy change; hence, the SAB-thrombin binding is driven by a favorable increase in entropy (Table).

We next analyzed the molecular structure of SAB (Figure 6A) and identified a striking structural similarity with the trisubstituted benzimidazole class of thrombin inhibitors, such as dabigatran (Figure 6B). Importantly, SAB possesses a benzofuran core group similar to that in the dabigatran benzimidazole backbone, which is essential for the structure-based design of thrombin inhibitors [57]. The main difference is that SAB has 2 side chains at positions 3 and 4 of the

benzofuran backbone. Using the resolved crystal structure of thrombin, we individually docked SAB and dabigatran to the thrombin active site using an *in silico* molecular docking model (Figure 6C, E), which showed several shared binding residues between SAB and dabigatran with the thrombin active site (Figure 6D, F).

Our results elucidate the inhibitory effect of SAB on the enzymatic activity of thrombin and explain its mechanism of action by sterically hindering the thrombin catalytic site. Thus, SAB can represent a robust and naturally available thrombin inhibitor with striking

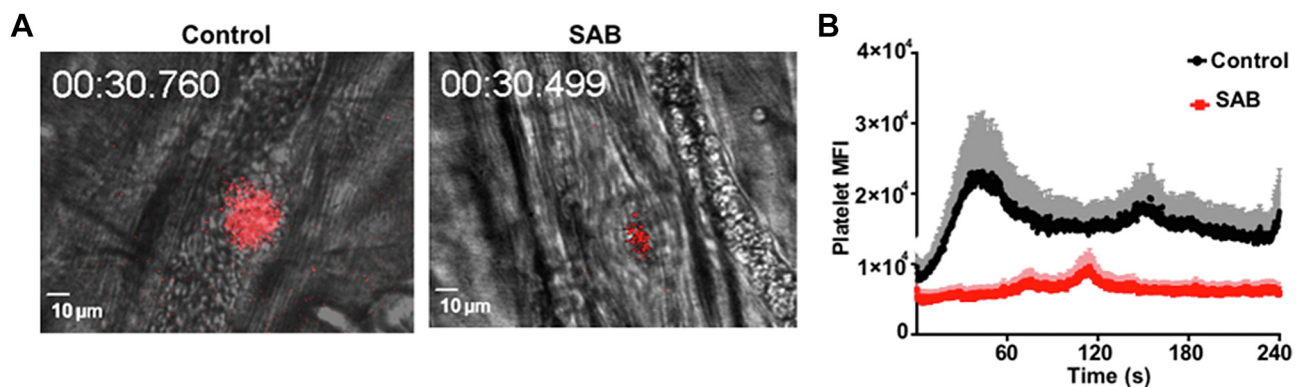


FIGURE 4 SAB inhibits thrombus formation *in vivo*. (A) Representative image of thrombus formation induced in a murine cremaster muscle laser injury model. The platelets were labeled in red. The scale bar denotes 10 microns. (B) SAB markedly reduced thrombus formation *in vivo* as shown by platelet MFI. $n = 4$. SAB was injected through the jugular vein cannula to a final *in vivo* concentration of 0.010 mM based on the weight of each mouse (80 µL/g total blood volume). MFI, mean fluorescence intensity; SAB, salvianolic acid B.

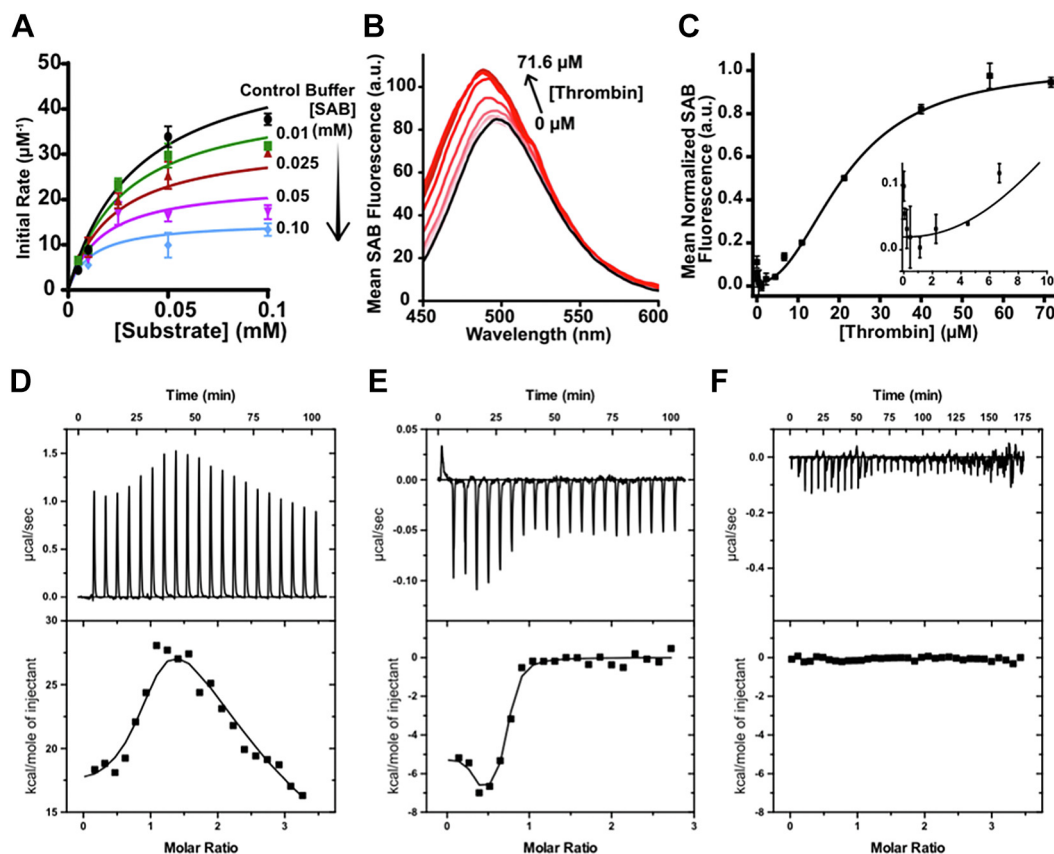


FIGURE 5 Direct binding of SAB to thrombin. (A) SAB directly inhibits the enzymatic activity of thrombin. Plot of initial rate vs substrate concentration at different SAB concentrations. Global Michaelis–Menten model (fit all curves to shared parameters). (B) Exhibits intrinsic fluorescence of 0.03 mM SAB (λ_{ex} 382 nm) titrated with thrombin in PBS (pH 7.4) at 20 °C. (C) Data obtained from the fluorescence binding detection assay were fit to our previously published binding script. Intrinsic fluorescence of SAB shows direct binding to thrombin. The inset displays a zoomed view of 2 binding events, quenching and enhancement. Characterization of thrombin binding to (D) SAB and (E) dabigatran using ITC. (F) Shows the ITC titration of SAB into control lysozyme solution, where no binding was observed. ITC reveals direct binding of SAB to thrombin. For each ITC panel, on top is the raw titration data demonstrating the heat resulting from each injection of ligand into protein solution. The bottom shows the integrated heat plot after correcting for the heat of dilution. Binding experiments were performed in PBS buffer (pH 7.4) at 20 °C. $n = 3$ to 4. ITC, isothermal titration calorimetry; PBS, phosphate-buffered saline; SAB, salvianolic acid B.

structural and functional similarities to the laboratory-designed trisubstituted benzimidazole class of thrombin inhibitors.

4 | DISCUSSION

In this study, we demonstrated, for the first time, that SAB inhibits blood coagulation through direct blocking of the thrombin active site. Our findings offered a novel mechanism to explain the potent inhibition of SAB on thrombin-induced platelet aggregation, activation, and thrombus formation *in vivo* (Figures 1–3). SAB, a compound derived

from an ancient herbal medicine, Danshen, shares striking structural similarities with the pharmacologically designed and biochemically synthesized trisubstituted benzimidazole class thrombin inhibitors. Our finding provides a new antithrombotic mechanism for SAB and establishes SAB as the first herb-derived direct thrombin inhibitor. In addition, SAB can inhibit platelet aggregation via thrombin-independent mechanisms (Supplementary Figure S1), which likely work synergistically with the thrombin blockage and result in a potent *in vivo* antithrombotic effect.

Danshen depside salt is one of the most widely used traditional Chinese medicine, and it has been prescribed to millions of patients in

TABLE Isothermal titration calorimetry binding affinities and thermodynamic properties of SAB and dabigatran interactions with thrombin^a.

Reagent	K_{d1} (nM)	ΔH_1 (kcal/mol)	$-T\Delta S_1$ (kcal/mol)	K_{d2} (nM)	ΔH_2 (kcal/mol)	$-T\Delta S_2$ (kcal/mol)	n_H
SAB	620 ± 80	18 ± 1	-27 ± 1	3700 ± 400	180 ± 6	-185 ± 12	1.1
Dabigatran	0.49 ± 0.16	-5.2 ± 0.6	-12 ± 1	24 ± 13	-7.4 ± 0.9	-4.9 ± 0.9	

K_{d1} and K_{d2} , dissociation constant; SAB, salvianolic acid B.

^aIsothermal titration calorimetry data were acquired at 20 °C in PBS buffer (pH 7.4). No binding was detected with SAB–lysozyme control under these experimental conditions.

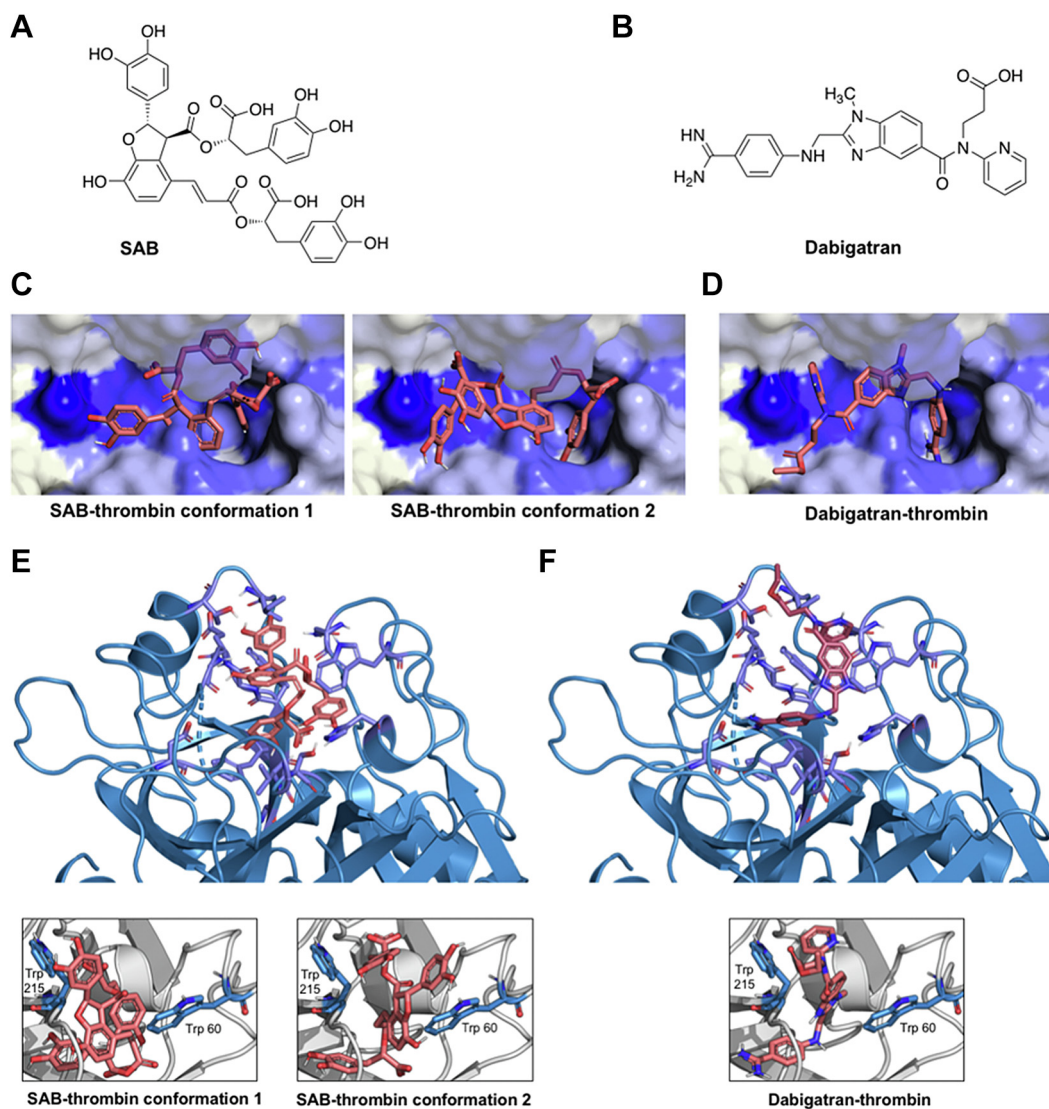


FIGURE 6 SAB occupies the 2-site binding pocket of the trisubstituted benzimidazole thrombin inhibitors. Molecular structure of SAB (A) and dabigatran (B). Thrombin binding pocket interactions with (C, E) SAB in red and (D, F) the inhibitor dabigatran in fuchsia resolved using computational docking analysis. The blue ribbon displays the published X-ray crystal structure of thrombin (PDB: 1KTS). Purple side chains show interacting residues with the bound ligands. SAB, salviainic acid B.

Asia and around the world [27]. The primary rationale for its use is the potent clinical antithrombotic effect. The low cost of Danshen depside salt makes it particularly attractive for the treatment of cardiovascular disease in developing countries. As the predominant ingredient of Danshen depside salt, SAB is considered the main active antithrombotic component. However, the mechanism of SAB in treating thrombosis is insufficiently explored, which significantly limits the understanding and study of its clinical benefits and risk profiles [63]. Previous studies focused on analyzing SAB and platelet receptor interactions and suggested that SAB targets platelet surface P2Y1, P2Y12, and $\alpha 2\beta 1$ integrin [29–31]. While these findings provide some explanations for the inhibitory effects of SAB in platelet aggregation, they are insufficient to elucidate the whole spectrum of its potent clinical antithrombotic outcome. Our data revealed a new perspective

on the antithrombotic function of SAB through direct inhibition of thrombin activity. Thrombin is a serine protease and one of the most potent platelet agonists through its proteolytic activation of platelet PAR1 and PAR2 receptors [19]. We showed that SAB exerted a more potent inhibitory effect and could abolish platelet aggregation when thrombin was used as an agonist, suggesting that the direct blocking of thrombin activity is a crucial mechanism of action for suppressing platelet aggregation.

The inhibition of SAB for *in vivo* thrombus formation, as observed in our intravital microscopy model (Figure 4A, B), is considerably more potent than observed in the *in vitro* and *ex vivo* experiments. Indeed, *in vitro* assays for cell-free plasma coagulation and platelet aggregation induced by a single agonist require a relatively high dose of SAB. This is likely due to a synergistic effect of action on platelet adhesion,

aggregation, and blood coagulation *in vivo*. The stable adhesion of platelets was mediated by integrins such as $\alpha 2\beta 1$ integrin, which was found to be targeted by SAB [31]. Additional platelet aggregation on the adhered platelets is mediated by platelet activation through the outside-in and inside-out signaling, with significant contributions from ADP and thrombin. SAB was reported to block ADP receptors P2Y1 and P2Y12 [29, 30], and our results showed that thrombin activity is also suppressed. In addition to its action on platelets, SAB suppressed the “second wave” of thrombus formation [30] by inhibiting fibrin clot formation on the initial platelet plug. This versatile inhibitory effect of SAB on multiple key steps of platelet thrombus formation and coagulation suggests that SAB may represent an efficient “one stone for two birds” strategy for both arterial and venous thrombosis therapy. In addition, mounting evidence indicates that thrombin promotes atherosclerotic plaque progression [64]. The established antiatherosclerosis function of Danshen extracts [65] can also be attributed to the inhibition of thrombin activity by SAB.

SAB, as the main component of Danshen, has been used in Asia for decades without a clear understanding of its pharmacologic mechanism of action. On the other hand, the trisubstituted benzimidazole class thrombin inhibitors, such as dabigatran, were designed by Boehringer Ingelheim in the early 2000s based on the crystal structure of thrombin [57]. It is, therefore, surprising to see that SAB and dabigatran share similar molecular structures and bind to similar residues in the thrombin active site. While the use of dabigatran is limited by its high cost, Danshen deposite salt is readily available and represents a common antithrombotic remedy used in China and other Asian countries. Although the inhibitory potency of SAB for thrombin activity was less than dabigatran, it was given at a high dose clinically through direct intravenous infusion [27].

The obtained thermodynamic parameters for SAB binding to thrombin showed that the enthalpy change of ligand binding is unfavorable, though this is counter-balanced by a favorable change in entropy (Table). Upon the formation of the SAB-thrombin complex, SAB and thrombin interact in a way that induces an increase in the entropy of the system, possibly due to the conformational changes in both SAB and thrombin. As a result, the complex can rearrange multiple orientations [66,67]. This increase in disorder contributes positively to the binding processes, where entropy serves as a driving factor that supports the stable binding of SAB to thrombin (Figure 5). These ITC data support the conformational change observed with our *in silico* molecular docking, where 2 conformers of SAB were yielded at this binding site (Figure 6). In addition to the favorable entropy, hydrophobic interactions can contribute to the overall binding affinity and stability of the SAB-thrombin complex [67,68]. We observed a Hill coefficient of 1.1 for the interaction between SAB and thrombin, indicating a positive cooperativity. This implies that the binding of the first interaction of the SAB with the thrombin catalytic cavity triggers a conformational change, facilitating a stronger binding for the second SAB-thrombin interaction.

Our study also explained the reason for a relatively high dose of SAB required for the clinical antithrombotic effect. Danshen deposite

salt (>85% made of SAB) is given clinically via intravenous (I.V.) injection at a daily dose of 200 mg (half-life of 2.87 hours and a median length of therapy period of 7 days) [69], which equals to >0.050 mM of plasma SAB concentration after each i.v. injection in 5.1 ± 0.8 L total blood volume in an average adult person. This clinical i.v. dosage and half-life are consistent with our observed *in vivo* effective dosage at ~ 0.010 mM (Figure 4). It is noticeable that this i.v. effect is achieved through a synergistic effect on thrombin-dependent and thrombin-independent mechanisms described above. The reduced thrombin-blockage potency (as compared with dabigatran) is likely due to the existence of the side chain catechol group on the benzofuran core structure, which interfered with the close contact of SAB with the thrombin active site (Figure 6). Removal of this side chain group may significantly enhance the efficacy of SAB in treating thrombosis. We also made the crucial finding that repeated freeze-thaw cycles and oxidation of SAB can change its potency (Supplementary Figure S2A–D), which should be a key consideration for prospective drug development.

In summary, our data established SAB as an herb-derived direct thrombin inhibitor that suppresses platelet activation, aggregation, and coagulation. The anticoagulation effect identified here provides critical mechanistic data for further investigations of the efficacy and safety of SAB in clinical use. The thrombin-dependent and thrombin-independent pathways may make SAB an attractive choice to synergistically block platelet adhesion, aggregation, and blood coagulation, which should significantly impact therapies against both arterial and deep vein thrombosis. Future chemical modifications may increase the anti-thrombin effect of SAB and broaden its application as an antithrombotic therapy.

ACKNOWLEDGMENTS

We would like to acknowledge the Keenan Research Centre for Biomedical Science Core Facilities at St Michael's Hospital (Toronto, Ontario, Canada). We thank the Hospital for Sick Children (Toronto, Ontario, Canada) for the use of the Structural & Biophysical Core Facility.

FUNDING

This work was funded by the Canadian Institutes of Health Research Foundation grant (389035, to H.N.). M.A.D.N., S.S., and A.A.S. are recipients of the Canadian Blood Services postdoctoral fellowship; T.N. and T.W.S. are recipients of the CIHR Canada Graduate Scholarships Masters Award. D.T.M. is a recipient of the Graduate Scholarship, Department of Physiology, University of Toronto, and Queen Elizabeth II Graduate Scholarship, Ontario, Canada; Y.W. is a recipient of the PhD Graduate Fellowship from Canadian Blood Services and Meredith & Malcolm Silver Scholarship in Cardiovascular Studies. A.A.S. is the recipient of the Graduate Scholarship Award, York University, Ontario, Canada. R.C.G. is the recipient of the National Sciences and Engineering Research Council of Canada (NSERC)—Canada Graduate Scholarships. P.E.J. is funded by an NSERC Discovery Grant.

ETHICS STATEMENT

All animal studies were approved by the Animal Care Committee of St Michael's Hospital, Toronto, Ontario, Canada. All experimental procedures using human plasma were approved by the Research Ethics Board of St Michael's Hospital, Toronto, Ontario, Canada.

AUTHOR CONTRIBUTIONS

M.A.D.N., T.N., D.T.M., and Y.W. designed the research studies, performed the experiments, analyzed data, generated the figures, and wrote the manuscript. A.A.S., X.L., S.S., S.Y., T.W.S., R.C.G., D.Z., X.R.X., C.F., and G.Z. performed the experiments, analyzed the data, and made critical revisions of the manuscript. L.W.D. and P.E.J. provided critical reagents and equipment, analyzed the data and made critical revision of the manuscript. K.C. and M.R. contributed to the development of the study concept and made critical revisions of the manuscript. Y.W. contributed to the supervision of the study. H.N. is the principal investigator who supervised the project, analyzed the data, and wrote and made critical revisions of the manuscript. All authors read and approved the final manuscript.

RELATIONSHIP DISCLOSURE

H.N., X.R.X., G.Z., X.L., M.A.D.N., and CCOA may have potential competing interests that may arise from the association with CCOA Therapeutics Inc. The other authors have no competing interests to disclose.

DATA AVAILABILITY

All data generated or analyzed during this study are included in this article (and its Supplementary material files).

REFERENCES

- [1] Collier BS. Historical perspective and future directions in platelet research. *J Thromb Haemost.* 2011;9:374–95.
- [2] Wang Y, Andrews M, Yang Y, Lang S, Jin JW, Cameron-Vendrig A, et al. Platelets in thrombosis and hemostasis: old topic with new mechanisms. *Cardiovasc Hematol Disord Drug Targets.* 2012;12:126–32.
- [3] Xu XR, Gallant RC, Ni H. Platelets, immune-mediated thrombocytopenias, and fetal hemorrhage. *Thromb Res.* 2016;141:S76–9.
- [4] Stronck DF, Rebullia P. Platelet transfusions. *Lancet.* 2007;370:427–38.
- [5] Ni H, Chen P, Spring CM, Sayeh E, Semple JW, Lazarus AH, et al. A novel murine model of fetal and neonatal alloimmune thrombocytopenia: response to intravenous IgG therapy. *Blood.* 2006;107:2976–83.
- [6] Yougbaré I, Lang S, Yang H, Chen P, Zhao X, Tai W-S, et al. Maternal anti-platelet $\beta 3$ integrins impair angiogenesis and cause intracranial hemorrhage. *J Clin Invest.* 2015;125:1545–56.
- [7] Ruggeri ZM. Platelets in atherothrombosis. *Nat Med.* 2002;8:1227–34.
- [8] Mackman N. Triggers, targets and treatments for thrombosis. *Nature.* 2008;451:914–8.
- [9] Davi G, Patrono C. Platelet activation and atherothrombosis. *N Engl J Med.* 2007;357:2482–94.
- [10] Xu XR, Zhang D, Oswald BE, Carrim N, Wang X, Hou Y, et al. Platelets are versatile cells: new discoveries in hemostasis, thrombosis, immune responses, tumor metastasis and beyond. *Crit Rev Clin Lab Sci.* 2016;53:409–30.
- [11] Jackson SP. Arterial thrombosis—insidious, unpredictable and deadly. *Nat Med.* 2011;17:1423–36.
- [12] Wang Y, Gallant RC, Ni H. Extracellular matrix proteins in the regulation of thrombus formation. *Curr Opin Hematol.* 2016;23:280–7.
- [13] Schmaier AH. Are maternal antiplatelet antibodies a prothrombotic condition leading to miscarriage? *J Clin Invest.* 2011;121:4241–3.
- [14] Li C, Piran S, Chen P, Lang S, Zarpellon A, Jin JW, et al. The maternal immune response to fetal platelet GPIIb/IIIa causes frequent miscarriage in mice that can be prevented by intravenous IgG and anti-FcRn therapies. *J Clin Invest.* 2011;121:4537–47.
- [15] Wendelboe AM, Raskob GE. Global burden of thrombosis: epidemiologic aspects. *Circ Res.* 2016;118:1340–7.
- [16] Key NS, Negrier C. Coagulation factor concentrates: past, present, and future. *Lancet.* 2007;370:439–48.
- [17] Pieters M, Wolberg AS. Fibrinogen and fibrin: an illustrated review. *Res Pract Thromb Haemost.* 2019;3:161–72.
- [18] Coughlin SR. Thrombin signalling and protease-activated receptors. *Nature.* 2000;407:258–64.
- [19] Nieman MT. Protease-activated receptors in hemostasis. *Blood.* 2016;128:169–77.
- [20] Han X, Nieman MT, Kerlin BA. Protease-activated receptors: an illustrated review. *Res Pract Thromb Haemost.* 2021;5:17–26.
- [21] Coppens M, Eikelboom JW, Gustafsson D, Weitz JI, Hirsh J. Translational success stories: development of direct thrombin inhibitors. *Circ Res.* 2012;111:920–9.
- [22] Hankey GJ, Eikelboom JW. Dabigatran etexilate: a new oral thrombin inhibitor. *Circulation.* 2011;123:1436–50.
- [23] Bancroft T, Lim J, Wang C, Sander SD, Swindle JP. Health care resource utilization, costs, and persistence in patients newly diagnosed as having nonvalvular atrial fibrillation and newly treated with dabigatran versus warfarin in the United States. *Clin Ther.* 2016;38:545–56.e6. <https://doi.org/10.1016/j.clinthera.2016.01.008>
- [24] Du G, Song J, Du L, Zhang L, Qiang G, Wang S, et al. Chemical and pharmacological research on the polyphenol acids isolated from Danshen: a review of salvianolic acids. *Adv Pharmacol.* 2020;87:1–41.
- [25] Ma W, Rousseau Z, Slavkovic S, Shen C, Yousef GM, Ni H. Doxorubicin-induced platelet activation and clearance relieved by salvianolic acid compound: novel mechanism and potential therapy for chemotherapy-associated thrombosis and thrombocytopenia. *Pharmaceuticals (Basel).* 2022;15:1444.
- [26] Li ZM, Xu SW, Liu PQ. Salvia miltiorrhiza Burge (Danshen): a golden herbal medicine in cardiovascular therapeutics. *Acta Pharmacol Sin.* 2018;39:802–24.
- [27] Writing Group of Recommendations of Expert Panel from Chinese Geriatrics Society on the Clinical Use of Compound Danshen Dripping Pills. Recommendations on the clinical use of compound Danshen dripping pills. *Chin Med J (Engl).* 2017;130:972–8.
- [28] Cao J, Wei YJ, Qi LW, Li P, Qian ZM, Luo HW, et al. Determination of fifteen bioactive components in Radix et Rhizoma *Salviae Miltiorrhizae* by high-performance liquid chromatography with ultraviolet and mass spectrometric detection. *Biomed Chromatogr.* 2008;22:164–72.
- [29] Liu L, Li J, Zhang Y, Zhang S, Ye J, Wen Z, et al. Salvianolic acid B inhibits platelets as a P2Y12 antagonist and PDE inhibitor: evidence from clinic to laboratory. *Thromb Res.* 2014;134:866–76.
- [30] Liu X, Gao ZG, Wu Y, Stevens RC, Jacobson KA, Zhao S. Salvianolic acids from antithrombotic traditional Chinese medicine Danshen are antagonists of human P2Y1 and P2Y12 receptors. *Sci Rep.* 2018;8:8084.
- [31] Wu YP, Zhao XM, Pan SD, Guo DA, Wei R, Han JJ, et al. Salvianolic acid B inhibits platelet adhesion under conditions of flow by a

- mechanism involving the collagen receptor alpha2beta1. *Thromb Res*. 2008;123:298–305.
- [32] Yang H, Reheman A, Chen P, Zhu G, Hynes RO, Freedman J, et al. Fibrinogen and von Willebrand factor-independent platelet aggregation in vitro and in vivo. *J Thromb Haemost*. 2006;4:2230–7.
- [33] Wang Y, Reheman A, Spring CM, Kalantari J, Marshall AH, Wolberg AS, et al. Plasma fibronectin supports hemostasis and regulates thrombosis. *J Clin Invest*. 2014;124:4281–93.
- [34] Xu XR, Wang Y, Adili R, Ju L, Spring CM, Jin JW, et al. Apolipoprotein A-IV binds α IIb β 3 integrin and inhibits thrombosis. *Nat Commun*. 2018;9:3608.
- [35] Shen C, MacKeigan DT, Shoara AA, Xu R, Bhorja P, Karakas D, et al. Dual roles of fucoidan-GPIIb α interaction in thrombosis and hemostasis: implications for drug development targeting GPIIb α . *J Thromb Haemost*. 2023;21:1274–88.
- [36] Byrnes JR, Duval C, Wang Y, Hansen CE, Ahn B, Mooberry MJ, et al. Factor XIIIa-dependent retention of red blood cells in clots is mediated by fibrin α -chain crosslinking. *Blood*. 2015;126:1940–8.
- [37] Nagrath M, Gallant R, Yazdi AR, Mendonca A, Rahman S, Chiu L, et al. Tantalum-containing mesoporous bioactive glass powder for hemostasis. *J Biomater Appl*. 2021;35:924–32.
- [38] Levy JH, Szlam F, Wolberg AS, Winkler A. Clinical use of the activated partial thromboplastin time and prothrombin time for screening: a review of the literature and current guidelines for testing. *Clin Lab Med*. 2014;34:453–77.
- [39] Gidley GN, Holle LA, Burthum J, Bolton-Maggs PHB, Lin FC, Wolberg AS. Abnormal plasma clot formation and fibrinolysis reveal bleeding tendency in patients with partial factor XI deficiency. *Blood Adv*. 2018;2:1076–88.
- [40] Li BX, Dai X, Xu XR, Adili R, Neves MAD, Lei X, et al. In vitro assessment and phase I randomized clinical trial of anfibatide a snake venom derived anti-thrombotic agent targeting human platelet GPIIb α . *Sci Rep*. 2021;11:11663.
- [41] Reheman A, Yang H, Zhu G, Jin W, He F, Spring CM, et al. Plasma fibronectin depletion enhances platelet aggregation and thrombus formation in mice lacking fibrinogen and von Willebrand factor. *Blood*. 2009;113:1809–17.
- [42] Zhu G, Zhang Q, Reddy EC, Carrim N, Chen Y, Xu XR, et al. The integrin PSI domain has an endogenous thiol isomerase function and is a novel target for antiplatelet therapy. *Blood*. 2017;129:1840–54.
- [43] Yang Y, Shi Z, Reheman A, Jin JW, Li C, Wang Y, et al. Plant food delphinidin-3-glucoside significantly inhibits platelet activation and thrombosis: novel protective roles against cardiovascular diseases. *PLoS One*. 2012;7:e37323. <https://doi.org/10.1371/journal.pone.0037323>
- [44] Wong C, Liu Y, Yip J, Chand R, Wee JL, Oates L, et al. CEACAM1 negatively regulates platelet-collagen interactions and thrombus growth in vitro and in vivo. *Blood*. 2009;113:1818–28.
- [45] Lei X, MacKeigan DT, Ni H. Control of data variations in intravital microscopy thrombosis models. *J Thromb Haemost*. 2020;18:2823–5.
- [46] Eltringham-Smith LJ, Lei X, Reheman A, Lambourne MD, Prydzial EL, Ni H, et al. The fibrinogen but not the factor VIII content of transfused plasma determines its effectiveness at reducing bleeding in coagulopathic mice. *Transfusion*. 2015;55:1040–50.
- [47] Lei X, Reheman A, Hou Y, Zhou H, Wang Y, Marshall AH, et al. Anfibatide, a novel GPIIb complex antagonist, inhibits platelet adhesion and thrombus formation in vitro and in vivo in murine models of thrombosis. *Thromb Haemost*. 2014;111:279–89.
- [48] Slavkovic S, Johnson PE. Analysis of aptamer-small molecule binding interactions using isothermal titration calorimetry. *Methods Mol Biol*. 2023;2570:105–18.
- [49] Ma X, Liang J, Zhu G, Bhorja P, Shoara AA, MacKeigan DT, et al. SARS-CoV-2 RBD and its variants can induce platelet activation and clearance: implications for antibody therapy and vaccinations against COVID-19. 6. Research (Wash D C); 2023:0124.
- [50] Freiburger LA, Auclair K, Mittermaier AK. Elucidating protein binding mechanisms by variable-c ITC. *ChemBioChem*. 2009;10:2871–3.
- [51] Freire E, Schön A, Velazquez-Campoy A. *Isothermal titration calorimetry: general formalism using binding polynomials*. Methods in Enzymology. Academic Press; 2009:127–55.
- [52] Cattoni DI, Chara O, Kaufman SB, González Flecha FL. Cooperativity in binding processes: new insights from phenomenological modeling. *PLoS One*. 2016;10:e0146043. <https://doi.org/10.1371/journal.pone.0146043>
- [53] Shoara AA, Slavkovic S, Donaldson LW, Johnson PE. Analysis of the interaction between the cocaine-binding aptamer and its ligands using fluorescence spectroscopy. *Canadian J Chem*. 2017;95:1253–60.
- [54] Shoara AA, Churcher ZR, Steele TWJ, Johnson PE. Analysis of the role played by ligand-induced folding of the cocaine-binding aptamer in the photochromic aptamer switch assay. *Talanta*. 2020;217:121022.
- [55] Bromfield KM, Quinsey NS, Duggan PJ, Pike RN. Approaches to selective peptidic inhibitors of factor Xa. *Chem Biol Drug Des*. 2006;68:11–9.
- [56] Trott O, Olson AJ. AutoDock Vina: improving the speed and accuracy of docking with a new scoring function, efficient optimization, and multithreading. *J Comput Chem*. 2010;31:455–61.
- [57] Huel NH, Nar H, Pripke H, Ries U, Stassen JM, Wiene W. Structure-based design of novel potent nonpeptide thrombin inhibitors. *J Med Chem*. 2002;45:1757–66.
- [58] Eisenberg D, Schwarz E, Komaromy M, Wall R. Analysis of membrane and surface protein sequences with the hydrophobic moment plot. *J Mol Biol*. 1984;179:125–42.
- [59] Johnson PE, Donaldson LW. RNA recognition by the Vts1p SAM domain. *Nat Struct Mol Biol*. 2006;13:177–8.
- [60] Li J, van der Wal DE, Zhu G, Xu M, Yougbare I, Ma L, et al. Desialylation is a mechanism of Fc-independent platelet clearance and a therapeutic target in immune thrombocytopenia. *Nat Commun*. 2015;6:7737.
- [61] Tao L, Zeng Q, Li J, Xu M, Wang J, Pan Y, et al. Platelet desialylation correlates with efficacy of first-line therapies for immune thrombocytopenia. *J Hematol Oncol*. 2017;10:46.
- [62] Weisel JW, Litvinov RI. Mechanisms of fibrin polymerization and clinical implications. *Blood*. 2013;121:1712–9.
- [63] Yu Y, Spatz ES, Tan Q, Liu S, Lu Y, Masoudi FA, et al. Traditional Chinese medicine use in the treatment of acute heart failure in Western medicine hospitals in China: analysis from the China PEACE Retrospective Heart Failure Study. *J Am Heart Assoc*. 2019;8:e012776. <https://doi.org/10.1161/jaha.119.012776>
- [64] Borissoff JI, Spronk HM, ten Cate H. The hemostatic system as a modulator of atherosclerosis. *N Engl J Med*. 2011;364:1746–60.
- [65] Wu YJ, Hong CY, Lin SJ, Wu P, Shiao MS. Increase of vitamin E content in LDL and reduction of atherosclerosis in cholesterol-fed rabbits by a water-soluble antioxidant-rich fraction of *Salvia miltiorrhiza*. *Arterioscler Thromb Vasc Biol*. 1998;18:481–6.
- [66] Starikov EB, Nordén B. Enthalpy–entropy compensation: a phantom or something useful? *J Phys Chem B*. 2007;111:14431–5.
- [67] Slavkovic S, Shoara AA, Churcher ZR, Daems E, de Wael K, Sobott F, et al. DNA binding by the antimalarial compound artemisinin. *Sci Rep*. 2022;12:133.
- [68] Chodera JD, Mobley DL. Entropy-enthalpy compensation: role and ramifications in biomolecular ligand recognition and design. *Annu Rev Biophys*. 2013;42:121–42.
- [69] Yan YY, Yang YH, Wang WW, Pan YT, Zhan SY, Sun MY, et al. Post-marketing safety surveillance of the *Salvia miltiorrhiza* depside salt for infusion: a real world study. *PLoS One*. 2017;12:e0170182. <https://doi.org/10.1371/journal.pone.0170182>

SUPPLEMENTARY MATERIAL

The online version contains supplementary material available at <https://doi.org/10.1016/j.rpth.2024.102443>